Geometric signature of complex synchronisation scenarios

2013 EPL 102 30007

(http://iopscience.iop.org/0295-5075/102/3/30007)

A Letters Journal Exploring the Frontiers of Physics

May 2013

EPL, **102** (2013) 30007 www.epljournal.org
doi: 10.1209/0295-5075/102/30007

Geometric signature of complex synchronisation scenarios

J. H. Feldhoff[1,2(a)], R. V. Donner[1], J. F. Donges[1,2,3], N. Marwan[1] and J. Kurths[1,2,4]

[1] *Potsdam Institute for Climate Impact Research - P.O. Box 60 12 03, 14412 Potsdam, Germany, EU*
[2] *Department of Physics, Humboldt University - Newtonstr. 15, 12489 Berlin, Germany, EU*
[3] *Stockholm Resilience Centre, Stockholm University - Kräftriket 2B, 11419 Stockholm, Sweden, EU*
[4] *Institute for Complex Systems and Mathematical Biology, University of Aberdeen Aberdeen AB24 3FX, UK, EU*

received 30 November 2012; accepted in final form 23 April 2013
published online 17 May 2013

PACS 05.45.Tp – Time series analysis
PACS 05.45.Xt – Synchronization; coupled oscillators
PACS 89.75.Hc – Networks and genealogical trees

Abstract – Synchronisation between coupled oscillatory systems is a common phenomenon in many natural as well as technical systems. Varying the coupling strength often leads to qualitative changes in the dynamics exhibiting different types of synchronisation. Here, we study the geometric signatures of coupling along with the onset of generalised synchronisation (GS) between two coupled chaotic oscillators by mapping the systems' individual as well as joint recurrences in phase space to a complex network. For a paradigmatic continuous-time model system, we show that the transitivity properties of the resulting joint recurrence networks display distinct variations associated with changes in the structural similarity between different parts of the considered trajectories. They therefore provide a useful new indicator for the emergence of GS.

This paper is dedicated to the 25th anniversary of the introduction of recurrence plots by Eckmann et al. (EPL, 4 (1987) 973).

Introduction. – In the last two decades, there has been a rising interest in studying synchronisation of coupled oscillatory systems [1,2]. Specifically, for chaotic oscillators, it has been recognised that different phenomena have to be distinguished: In case of complete synchronisation (CS) [3] the trajectories $x(t)$ and $y(t)$ of the two coupled systems become identical ($y(t) = x(t)$), which is only possible for identical systems with a sufficiently strong coupling. Generalised synchronisation (GS) [4–7] refers to a general fixed and deterministic functional relationship between both trajectories, $y(t) = f(x(t))$, where f is a diffeomorphism. GS can occur for non-identical chaotic oscillators at moderate coupling strengths. A closely related form is lag synchronisation (LS) [8], where both coupled systems evolve in an identical way with a fixed mutual time shift as $y(t) = x(t - \tau)$. Finally, phase synchronisation (PS) [9] between non-identical systems typically arises at lower coupling strengths and is characterised by a locking between the phases of two systems, $m\phi_y(t) = n\phi_x(t)$ with $m, n \in \mathbb{N}$, whereas the amplitudes remain uncorrelated.

The sequence of synchronisation phenomena between two coupled oscillators with increasing coupling strength depends on their structural difference and specific coupling configuration. Typically, the dynamics of both systems becomes successively synchronised on more and more characteristic time-scales as the coupling strength increases [10,11]. This implies the emergence of PS at relatively low coupling strengths if the characteristic oscillation frequencies of both systems are sufficiently similar, whereas LS, GS, and CS typically occur at higher coupling strengths. However, the observed synchronisation scenario can also be much more complex.

A mathematical description of GS has been given first for driver-response systems. However, GS is not unique to systems with unidirectional coupling, but can be observed also for symmetrically coupled oscillators [12,13]. For driver-response relationships, the driven system undergoes systematic changes in its dynamical evolution as the coupling strength is increased. These changes can be

(a) E-mail: feldhoff@pik-potsdam.de

detected by a variety of methods such as the auxiliary system method [5], numerical estimates of the conditional Lyapunov exponent of the response system as a measure for its asymptotic stability [6], or by quantifying the predictability of the driven system. The latter class of approaches includes several methods based on neighbourhood relationships in phase space (*i.e.*, relying on geometric information), with the mutual false nearest-neighbour method [4] and the synchronisation likelihood [14] as most prominent examples. However, these methods are not always directly transferable to the case of bidirectional coupling configurations. Consequently, recently several new approaches have been proposed for studying GS for both uni- and bidirectional couplings, including methods based on recurrence plots [15] or a generalised angle between the trajectories of both systems [16].

Since synchronisation has distinct effects on the spatial organisation of driven systems in phase space, geometric methods are promising and widely applicable candidates for detecting GS from time series data. In this work we propose a new geometric method based on a complex network approach. Specifically, our method is based on a graph-theoretical interpretation of joint recurrence plots describing the simultaneous occurrence of mutually close pairs of state vectors in two or more coupled systems [17]. After presenting the details of our approach, we discuss the paradigmatic example of two coupled Rössler oscillators in different dynamical regimes in order to demonstrate the performance of the proposed method.

Methodology. – In the last years, the well-established framework of complex network theory [18,19] has become the basis for novel approaches of nonlinear time series analysis characterising complex systems [20–22] from a unique structural perspective. As a specific class of such time series networks, approaches characterising the mutual proximity of state vectors in phase space have become increasingly popular, since the resulting networks' structures reflect non-trivial geometric properties of the supposed (low-dimensional) attractor underlying the observed dynamics. A particularly interesting method are *recurrence networks* (RNs) [23–25], which encode the mutual proximity of state vectors in phase space arising from dynamical recurrences in the sense of Poincaré. Specifically, defining neighbourhoods of individual states by considering a spatial threshold distance ε around each observed state vector offers a flexible way for capturing the geometric backbone of the system under study. Formally, the system's finite-time recurrence properties infered from a time series $\{x_i\}_{i=1}^N$ are then represented by the binary *recurrence matrix*

$$R_{ij}(\varepsilon) = \Theta(\varepsilon - \|x_i - x_j\|), \tag{1}$$

where $\|\cdot\|$ is the maximum norm in phase space (however, other norms could be used here as well), and $\Theta(\cdot)$ denotes the Heaviside function. The visualisation of (R_{ij}) is commonly refered to as the *recurrence plot* [26] and has become an important tool for nonlinear time series analysis in the last decades [27].

RN analysis reinterprets eq. (1) as the adjacency matrix of an undirected simple graph defined as $A_{ij}(\varepsilon) = R_{ij}(\varepsilon) - \delta_{ij}$ (where δ_{ij} is Kronecker's delta). The resulting networks' properties can be described analytically by interpreting RNs as random spatial graphs with the system's invariant density uniquely determining RN connectivity [28,29]. This solid theoretical foundation allows using RNs for detecting dynamical changes in non-stationary time series from mathematical models as well as real-world applications [30–32]. One basic, yet important characteristic of RNs is the edge density $\rho(\varepsilon) = \sum_{i,j} A_{ij}(\varepsilon)/[N(N-1)]$, which is a monotonous function of ε [33]. In general, a suitable resolution of small-scale network features requires the choice of a low edge density (typically $\rho \lesssim 0.05$ [29,33]) with $\rho > \rho(\varepsilon_c)$, where ε_c is the percolation threshold of the RN [29].

The transitivity properties of RNs provide some particularly useful characteristics measuring the effective dimensionality of the underlying dynamical system in terms of the transitivity dimension [28]

$$D_{\mathcal{T}}(\varepsilon) = \frac{\log \mathcal{T}(\varepsilon)}{\log(3/4)} \tag{2}$$

based on the network transitivity [19,34]

$$\mathcal{T}(\varepsilon) = \frac{\sum_{i,j,k} A_{ij}(\varepsilon) A_{jk}(\varepsilon) A_{ki}(\varepsilon)}{\sum_{i,j,k} A_{ij}(\varepsilon) A_{ki}(\varepsilon)}. \tag{3}$$

This dimensionality interpretation of $\mathcal{T}$ is the foundation of the approach to studying geometric signatures of synchronisation to be detailed below. Other global RN characteristics (*e.g.*, average path length $\mathcal{L}$ or global clustering coefficient $\mathcal{C}$) have also proven their capabilities [23,25], but shall not be further discussed here for brevity.

Motivated by the great potentials of RN analysis of individual dynamical systems, a thorough extension to studying the collective dynamics of two or more coupled systems based on the concept of cross-recurrence plots [35] has been recently proposed [36]. However, the latter approach requires systems sharing the same phase space (a condition which is often not met in real-world applications) and is restricted to studying weakly unidirectionally coupled systems before the onset of GS [36]. In turn, in order to study the geometric signatures accompanying the onset of GS in some more detail, in this work we utilise another multivariate generalisation of the recurrence plot concept, *joint recurrence plots* [17], capturing the simultaneous occurrence of recurrences in two dynamical systems (fig. 1). The underlying *joint recurrence matrix*

$$JR_{ij}(\varepsilon_x, \varepsilon_y) = \Theta(\varepsilon_x - \|x_i - x_j\|)\Theta(\varepsilon_y - \|y_i - y_j\|) \tag{4}$$

is defined as the point-wise product of the individual systems' recurrence matrices. This basic concept can be directly generalised to the study of $K > 2$ coupled systems.

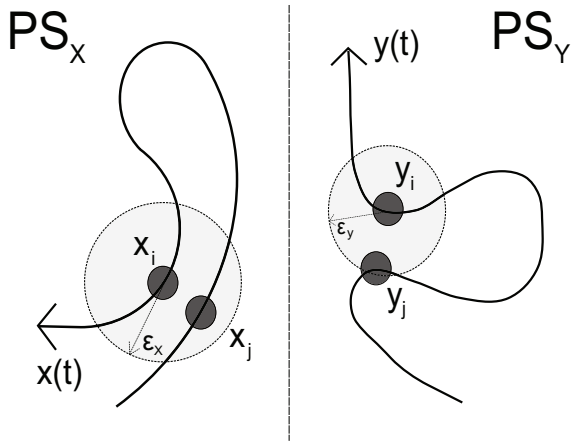

Fig. 1: Schematic illustration of a joint recurrence of two dynamical systems X and Y in their respective phase spaces PS_X and PS_Y.

Next, as for the traditional RN we reinterpret the joint recurrence matrix as the adjacency matrix of a so-called *joint recurrence network* (JRN) by setting $A_{ij}(\varepsilon_x, \varepsilon_y) = JR_{ij}(\varepsilon_x, \varepsilon_y) - \delta_{ij}$. JRNs can be constructed for systems with different phase spaces, but explicitly require simultaneous observations of all systems and, thus, time series of the same length. The system-specific thresholds ε_k should be chosen such that the edge densities $\rho_k(\varepsilon_k)$ of the RNs of the individual systems are fixed at the same value ρ to ensure comparability between the two considered systems, since the specific values of their RN properties typically depend on the chosen edge density [24,28]. By varying ρ, a reasonable JRN edge density $\rho_J \leq \rho$ can be obtained.

The properties of JRNs can be widely interpreted in a similar way as those of a classical RN in the higher-dimensional phase space of the composed system, with the exception that spatial proximity is evaluated separately in the subspaces belonging to the individual systems. Specifically, the transitivity $\mathcal{T}(\varepsilon_x, \varepsilon_y)$ (cf. eq. (3)) of the JRN (or, for short, *joint transitivity* $\mathcal{T}_J$) provides a measure for the "joint dimensionality" of the composed dynamical system (in a general sense). Due to the larger effective dimensionality of the joint phase space, for two systems X and Y in the absence of synchronisation we expect $\mathcal{T}_X, \mathcal{T}_Y \gtrsim \mathcal{T}_J$ (specifically, $D_{\mathcal{T}_J} = \log \mathcal{T}_J / \log(3/4) \approx D_{\mathcal{T}_X} + D_{\mathcal{T}_Y}$, cf. eq. (2)). In turn, when both systems exhibit GS, the effective degrees of freedom of both systems become mutually locked, resulting in $\mathcal{T}_J \to \mathcal{T}_X, \mathcal{T}_Y$, *i.e.*, both systems acting collectively as one with the same effective dimensionality as the individual systems. Consequently, studying the *transitivity ratio*

$$Q_{\mathcal{T}} = \frac{\mathcal{T}_J}{(\mathcal{T}_X + \mathcal{T}_Y)/2} \tag{5}$$

between the joint transitivity and the arithmetic mean of the individual systems' RN transitivities provides a purely geometric indicator for the emergence of GS. Note that for non-identical systems exhibiting GS, we still expect $\mathcal{T}_X \neq \mathcal{T}_Y$ due to subtle differences in the individual attractors' geometric shapes, so that we do not necessarily have $Q_{\mathcal{T}} \leq 1$ (see figs. 2 and 3). However, for structurally similar systems, $\mathcal{T}_X \approx \mathcal{T}_Y$ and, thus, $Q_{\mathcal{T}} \approx 1$ for GS.

Results. – As a well-studied paradigmatic model exhibiting different types of synchronisation phenomena, we study the performance of JRNs for two non-identical Rössler oscillators [37]

$$\begin{aligned}
\dot{x_1} &= -(1+\nu)x_2 - x_3, \\
\dot{x_2} &= (1+\nu)x_1 + a_x x_2 + \mu_{YX}(y_2 - x_2), \\
\dot{x_3} &= b_x + x_3(x_1 - c_x), \\
\dot{y_1} &= -(1-\nu)y_2 - y_3, \\
\dot{y_2} &= (1-\nu)y_1 + a_y y_2 + \mu_{XY}(x_2 - y_2), \\
\dot{y_3} &= b_y + y_3(y_1 - c_y),
\end{aligned} \tag{6}$$

that are diffusively coupled via their second component as in [15]. The detuning parameter ν accounts for a frequency mismatch of the nonlinear oscillations exhibited by both systems, making them non-identical even if $a_x = a_y = a$, $b_x = b_y = b$ and $c_x = c_y = c$ and, thus, prone to GS. In the following, we will keep $\nu = 0.02$ fixed. In turn, for the characteristic parameters a, b and c, we will mainly keep the same parameters for both systems throughout all further considerations. Specifically, we study the geometric signatures of the complex synchronisation scenarios arising for two different dynamical regimes with chaotic oscillations: the phase-coherent regime ($a = 0.16, b = 0.1, c = 8.5$) and the non–phase-coherent funnel regime ($a = 0.2925, b = 0.1, c = 8.5$). We integrate the coupled system with step size $h = 0.001$ until $T = 10000$, *i.e.*, for 10000000 time steps. In order to ensure that even very long transients are discarded, only data obtained for $T \geq 1,000$ are used for estimating the Lyapunov spectrum using the Wolf algorithm [38]. In a similar way, for estimating the RN properties only the interval $T \in [5000, 6000]$ is considered. The corresponding 1000000 time steps are downsampled by a factor of 200 to obtain RNs and JRNs with $N = 5000$ vertices. For comparative purposes, we also consider the recurrence plot-based indices CPR and JPR [15]. CPR, an indicator for PS, is based on the cross-correlation between the two systems' recurrence-based generalised auto-correlation functions, whereas JPR attempts to identify synchronisation by comparing the systems' RN edge densities $\rho_{X,Y}$ to ρ_J, which become very similar in case of GS.

Let us first examine a unidirectional coupling configuration $X \to Y$ ($\mu_{YX} = 0$), where the slightly faster system X drives the slower one Y. For two phase-coherent Rössler systems (fig. 2(A)), we find that when increasing the coupling strength μ_{XY} beyond about 0.06, the fourth-largest Lyapunov exponent λ_4 turns negative. At about the same value, CPR starts increasing indicating the possible onset of PS. At $\mu_{XY} \approx 0.17$, the third-largest Lyapunov exponent λ_3 becomes significantly negative, which is commonly interpreted as an indicator for the

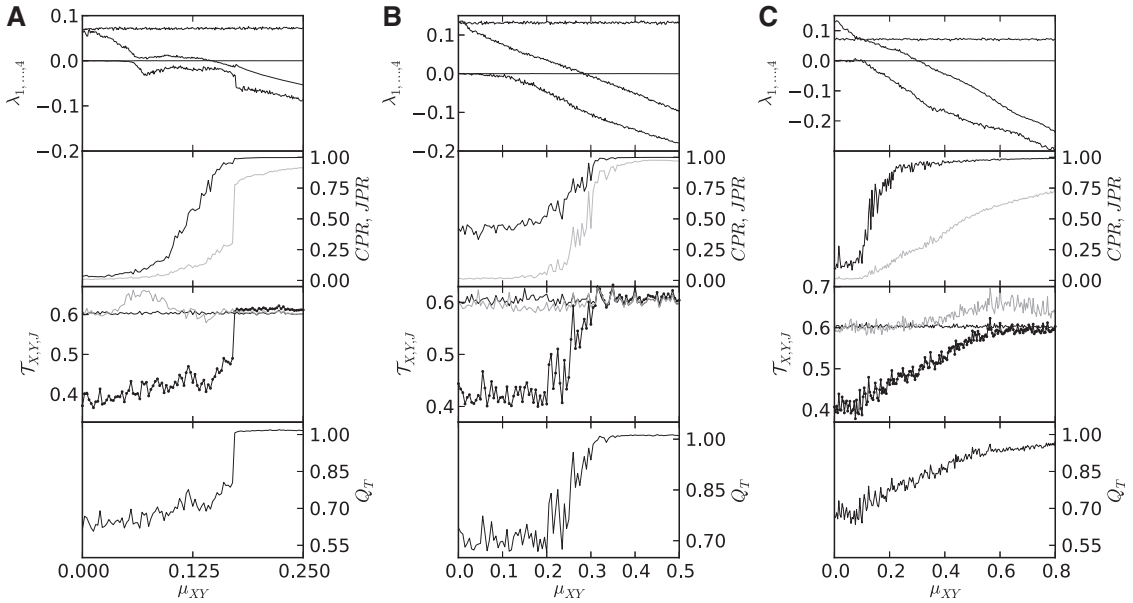

Fig. 2: Results of synchronisation analysis for two unidirectionally ($X \to Y$) coupled Rössler systems being (A) both in the phase-coherent regime, (B) both in the funnel regime, and (C) in phase-coherent (X) and funnel regime (Y): estimates of the four largest Lyapunov exponents $\lambda_1, \dots, \lambda_4$ (note that one of the Lyapunov exponents is always equal to zero due to the imposed coupling); recurrence-based synchronisation indices CPR (black) and JPR (grey) [15]; transitivities of individual and joint recurrence networks $\mathcal{T}_X$ (dark grey), $\mathcal{T}_Y$ (light grey) and $\mathcal{T}_J$ (black); transitivity ratio $Q_{\mathcal{T}}$ (from top to bottom).

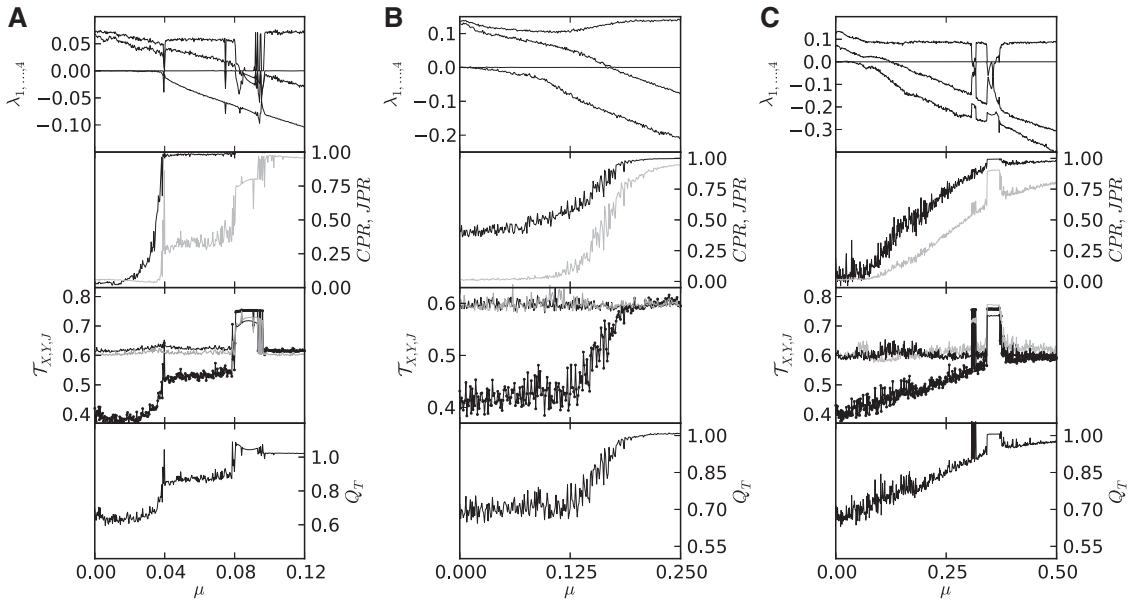

Fig. 3: As in fig. 2 for bidirectional coupling.

onset of GS. At the same time, we observe a sharp rise of JPR towards values of about 0.8, whereas $Q_{\mathcal{T}}$ immediately rises to values close to 1 (in fact, there is some weak overshooting because i) both systems are not fully identical and ii) the edge densities of RNs and JRN differ necessarily, resulting in slightly different estimates of the corresponding network transitivities).

The results are qualitatively similar when studying the same coupling configuration with both systems being in the non-coherent funnel regime (fig. 2(B)). Here, λ_4 becomes negative already at rather low coupling strengths, whereas $\lambda_3 < 0$ for $\mu_{XY} \approx 0.3$. The corresponding emergence of GS is accompanied by a continuous transition of JPR and $Q_{\mathcal{T}}$ to values of about 1, where $Q_{\mathcal{T}}$ again shows better convergence. Moreover, for symmetric bidirectionally coupled funnel systems ($\mu_{XY} = \mu_{YX} = \mu$, fig. 3(B)), we observe qualitatively the same behaviour as in the unidirectional case, with the corresponding

transitions taking place at smaller values of the coupling strength (*i.e.*, $\lambda_4 < 0$ for $\mu \gtrsim 0.02$ and $\lambda_3 < 0$ for $\mu \gtrsim 0.17$ [15]). Notably, the transition to GS as unveiled by both JPR and $Q_{\mathcal{T}}$ is even more continuous than for unidirectional coupling, and the residual difference of JRN to the ideal value of 1 close to the transition point is even larger, whereas $Q_{\mathcal{T}}$ is at the same time already very close to 1.

Studying two symmetrically coupled phase-coherent Rössler systems (fig. 3(A)), the synchronisation scenario gets more complex as μ is varied. Specifically, we find a small window close to the onset of PS at about $\mu = 0.039$, where CPR shows a sharp rise to values close to 1 [15]. The consistent signatures of the different GS indicators, together with the behaviour of the Lyapunov spectrum in this window, indicates the presence of (possibly intermittent) GS. At $\mu \gtrsim 0.04$, also JPR and $Q_{\mathcal{T}}$ increase considerably, reaching plateau values in the phase-synchronised chaotic regime [15]. For $\mu \in [0.08, 0.092]$, we find a more extended window of apparently periodic dynamics ($\lambda_2 < 0$) that probably corresponds to a regime of intermittent lag synchronisation [15], whereas for even larger coupling strength, we infer the presence of GS since $\lambda_3 < 0$, $JPR \approx 1$ and $Q_{\mathcal{T}} \approx 1$.

In order to illustrate the limitations of the proposed approach as well as the established JPR index, we finally study the signatures of synchronisation for the mixed case of a phase-coherent Rössler system X coupled to a funnel oscillator Y, which can be taken as an example for synchronisation between two strongly non-identical systems. In the case of unidirectional coupling (fig. 2(C)), we find $\lambda_4 < 0$ for $\mu_{XY} \gtrsim 0.1$ accompanied by an increase of CPR indicating the presence of PS. At $\mu_{XY} \approx 0.3$, also λ_3 approaches negative values, whereas both JPR and $Q_{\mathcal{T}}$ increase gradually, but do not approach values close to 1 even for relatively high coupling strengths. Thus, the three possible GS indicators λ_3, JPR and $Q_{\mathcal{T}}$ do not give consistent results in this case, which implies that we cannot unambigously conclude the possible presence of GS here. A similar statement holds for the bidirectional case (fig. 3(C)), which displays again a more complicated sequence of transitions.

We emphasise that the results described above remain still valid for considerably shorter time series lengths (*e.g.*, for $N = 500$) and in the presence of moderate levels (*e.g.*, about 5–10% of the signals standard deviation) of additive Gaussian white noise (not shown). These findings indicate a reasonable robustness of our method and its general applicability to real-world time series, which are often short and display observational noise of similar magnitude. It should be noted, that for such observational data, there is usually no possibility to vary the coupling strength between the considered systems. However, we conjecture that when knowing the individual systems' RN transitivities as well as their joint transitivity, one can still derive information on the presence or absence of GS. For this purpose, sophisticated significance tests need to be developed. A more detailed study of the aforementioned aspects is outlined for future work.

Conclusions. – 25 years after the introduction of recurrence plots by Eckmann *et al.* [26], the development of recurrence-based techniques still continues. With this paper, we would like to honour the seminal work by these authors and show how the paradigms of recurrence plots and complex networks have meanwhile been combined to pave the way for new concepts in complex systems analysis.

We have introduced a new fully geometric approach for detecting GS between two coupled chaotic oscillators based on time series data. Specifically, we have used a complex network interpretation of the recurrence as well as joint recurrence matrices, the transitivity properties of which allow tracing changes in the effective dimensionality of the individual system's attractors as well as the attractor of the combined higher-dimensional system. We have demonstrated that in the presence of GS, both systems effectively behave as one, with the dimensionality of the composed system approaching that of the individual ones.

For the case of structurally similar systems such as slightly detuned chaotic oscillators with otherwise equal characteristic parameters, we have shown that the ratio $Q_{\mathcal{T}}$ between the JRN transitivity and the arithmetic mean of the individual systems' RNs transitivities quickly approaches a value of 1 as GS takes place. In comparison with the conceptually related measure JPR, our geometric characteristic $Q_{\mathcal{T}}$ displays a better convergence to values close to 1 expected for GS. We relate this finding to the fact that $Q_{\mathcal{T}}$ captures higher-order dynamical characteristics, whereas JPR does not. Note that for structurally different systems, both indices fail to clearly indicate the transition to GS as unveiled by studying the Lyapunov spectrum.

In general, the proposed method has the advantage of being applicable to relatively short time series of length $N \lesssim \mathcal{O}(10^3)$, whereas the computational requirements for numerically estimating the Lyapunov spectrum are far higher and usually not met in case of real-world applications. In this spirit, we conclude that the proposed method has great potentials for future applications to observational data from different fields of research.

* * *

This work has been financially supported by the IRTG 1740/ TRP 2011/50151-0 (funded by the DFG/FAPESP), the Leibniz Society (project ECONS), the German National Academic Foundation, and the Potsdam Research Cluster for Georisk Analysis, Environmental Change and Sustainability (PROGRESS, support code 03IS2191B). For calculations of complex network measures, the software package `pyunicorn` has been used on the IBM iDataPlex Cluster of the Potsdam Institute for Climate Impact Research. We thank two anonymous referees

for their helpful comments on the initial version of this manuscript.

REFERENCES

[1] Pikovsky A., Rosenblum M. and Kurths J., *Synchronization – A Universal Concept in Nonlinear Sciences* (Cambridge University Press) 2001.

[2] Boccaletti S., Kurths J., Osipov G., Valladares D. L. and Zhou C. S., *Phys. Rep.*, **366** (2002) 1.

[3] Pecora L. M. and Carroll T. L., *Phys. Rev. Lett.*, **64** (1990) 821.

[4] Rulkov N. F., Sushchik M. M., Tsimring L. S. and Abarbanel H. D. I., *Phys. Rev. E*, **51** (1995) 980.

[5] Abarbanel H. D. I., Rulkov N. F. and Sushchik M. M., *Phys. Rev. E*, **53** (1996) 4528.

[6] Kocarev L. and Parlitz U., *Phys. Rev. Lett.*, **76** (1996) 1816.

[7] Boccaletti S., Valladares D. L., Kurths J., Maza D. and Mancini H., *Phys. Rev. E*, **61** (2000) 3712.

[8] Rosenblum M. G., Pikovsky A. S. and Kurths J., *Phys. Rev. Lett.*, **78** (1997) 4193.

[9] Rosenblum M. G., Pikovsky A. S. and Kurths J., *Phys. Rev. Lett.*, **76** (1996) 1804.

[10] Hramov A. E. and Koronovskii A. A., *Chaos*, **14** (2004) 603.

[11] Hramov A. E. and Koronovskii A. A., *Physica D*, **206** (2005) 252.

[12] Afraimovich V. S., Verichev N. N. and Rabinovich M. I., *Radiophys. Quantum Electron.*, **29** (1986) 795.

[13] Zheng Z., Wang X. and Cross M. C., *Phys. Rev. E*, **65** (2002) 056211.

[14] Stam C. and van Dijk B., *Physica D*, **163** (2002) 236.

[15] Romano M. C., Thiel M., Kurths J., Kiss I. Z. and Hudson J. L., *Europhys. Lett.*, **71** (2005) 466.

[16] Liu Z., Zhou J. and T. Munakata, *EPL*, **87** (2009) 50002.

[17] Romano M. C., Thiel M., Kurths J. and von Bloh W., *Phys. Lett. A*, **330** (2004) 214.

[18] Albert R. and Barabasi A.-L., *Rev. Mod. Phys.*, **74** (2002) 47.

[19] Newman M. E. J., *SIAM Rev.*, **45** (2003) 167.

[20] Zhang J. and Small M., *Phys. Rev. Lett.*, **96** (2006) 238701.

[21] Xu X., Zhang J. and Small M., *Proc. Natl. Acad. Sci. U.S.A.*, **105** (2008) 19601.

[22] Lacasa L., Luque B., Ballesteros F., Luque J. and Nuno J. C., *Proc. Natl. Acad. Sci. U.S.A.*, **105** (2008) 4972.

[23] Marwan N., Donges J. F., Zou Y., Donner R. V. and Kurths J., *Phys. Lett. A*, **373** (2009) 4246.

[24] Donner R. V., Zou Y., Donges J. F., Marwan N. and Kurths J., *New J. Phys.*, **12** (2010) 033025.

[25] Donner R. V., Small M., Donges J. F., Marwan N., Zou Y., Xiang R. and Kurths J., *Int. J. Bifurcat. Chaos*, **21** (2011) 1019.

[26] Eckmann J.-P., Kamphorst S. O. and Ruelle D., *Europhys. Lett.*, **4** (1987) 973.

[27] Marwan N., Romano M. C., Thiel M. and Kurths J., *Phys. Rep.*, **438** (2007) 237.

[28] Donner R. V., Heitzig J., Donges J. F., Zou Y., Marwan N. and Kurths J., *Eur. Phys. J. B*, **84** (2011) 653.

[29] Donges J. F., Heitzig J., Donner R. V. and Kurths J., *Phys. Rev. E*, **85** (2012) 046105.

[30] Donges J. F., Donner R. V., Rehfeld K., Marwan N., Trauth M. H. and Kurths J., *Nonlinear Proc. Geophys.*, **18** (2011) 545.

[31] Donges J. F., Donner R. V., Trauth M. H., Marwan N., Schellnhuber H. J. and Kurths J., *Proc. Natl. Acad. Sci. U.S.A.*, **108** (2011) 20422.

[32] Zou Y., Donner R. V., Wickramasinghe M., Kiss, I. Z., Small M. and Kurths J., *Chaos*, **22** (2012) 033130.

[33] Donner R. V., Zou Y., Donges J. F., Marwan N. and Kurths J., *Phys. Rev. E*, **81** (2010) 015101(R).

[34] Boccaletti S., Latora V., Moreno Y., Chavez M. and Hwang D.-U., *Phys. Rep.*, **424** (2006) 175.

[35] Marwan N. and Kurths J., *Phys. Lett. A*, **302** (2002) 299.

[36] Feldhoff J. H., Donner R. V., Donges J. F., Marwan N. and Kurths J., *Phys. Lett. A*, **376** (2012) 3504.

[37] Rössler O. E., *Phys. Lett. A*, **57** (1976) 397.

[38] Wolf A., Swift J. B., Swinney H. L. and Vastano J. A., *Physica D*, **16** (1985) 285.